Aggregation and Gel Formation in Basic Silico−Calco−Alkaline Solutions Studied: A SAXS, SANS, and ELS Study

Fabien Gaboriaud,* André Nonat, and Denis Chaumont

Laboratoire de Recherches sur la Réactivité des Solides (UMR 5613), Université de Bourgogne, 9 av Alain Savary BP47870−21078 Dijon Cedex, France

Aldo Craievich

Instituto de Física, Universidade de São Paulo, São Paulo, Brazil

Received: January 11, 1999; In Final Form: May 12, 1999

Gelation of strongly basic silico−alkaline solutions was promoted by appropriate additions of calcium ions. The structure of the aggregates formed in the precursor sols and the resulting gels were studied, within a wide length scale, using small-angle X-ray, small-angle neutron, and elastic light scattering. The study of the kinetics of aggregation was performed in situ. The experimental results demonstrate that gels are composed of aggregates exhibiting a fractal structure, large particles formed in the solutions just after calcium addition and, in some cases, small primary particles remaining in the solution phase. The structural features of the gels are strongly dependent on the concentration of calcium ions. Reaction limited aggregation and diffusion-limited aggregation of primary silicate species are the predominant mechanisms of aggregation and gel formation in solutions with low and high calcium concentration, respectively.

I. Introduction

The chemical processes involved in the formation of silica gels and silica powders focused the attention of many scientists in the past decades because of their important role in industrial production of new silica-based materials. Silica materials can be prepared by acidification of concentrated solutions of silica and sodium hydroxide precursors usually called water glass. These solutions are composed of silicate species (tetraedric monomers or small oligomers). The degree of polymerization depends on the pH of the solution and also on silica content.[1] The decrease in pH induces the formation of cyclic oligomers in the solution followed by the growth of primary particles. If the concentration number of these particles is high enough, i.e., if silica content in water glass is sufficiently high, the growing aggregates percolate and form a gel. The condensation reaction is described by[1,2]

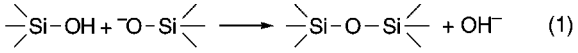

(1)

To understand the role of reaction conditions (temperature, pH, concentrations, salt addition) on the structure of the precursor sols and final gels, a number of investigations were performed. The mechanism of aggregation and the structure of the final gels were studied for pH values ranging from 2 to 10 which leads to a three-dimensional silica tetraedra network.[3,4]

Silica gels with high pH values, above 10, can be obtained by adding calcium ions to water glass solutions.[5,6] Provided silica concentration is high enough, a gel is obtained even under this strongly basic condition. Cracking effects observed in concrete have been attributed to the existence of microphases composed of this type of gels. The chemical process involved in the formation of these gels in that case is called alkali−silica reaction (ASR). This reaction is promoted the interaction between ions existing in the solution contained in the pores of concrete (hydroxides, calcium, sodium, potassium, and silicate) and the reactive silica of aggregates. A more detailed description of ASR reaction can be found in earlier publications.[7−9]

The process leading to "basic silica gels" also involves the formation of siloxane bonds. A previous work[10] showed that the formation of these bonds is induced by calcium ions in two steps. First, calcium ion forms a bond with one silicate species, which contains one ionized silanols (SiO^-), as illustrated in reaction 2.

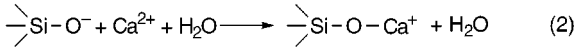

(2)

In the second step, this positive charge attracts a second silicate species. It forms an intermediary complex, which contains a bridge between two different silicate species induced by calcium ions. This unstable complex leads to the formation of a siloxane bond by ejecting calcium ion as illustrated in reaction 3.

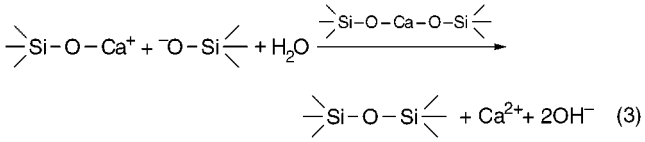

(3)

These two reactions show the enhancing action of calcium ions on the formation of siloxane bond. Nevertheless, this process does not exclude the formation of siloxane bonds through reaction 1.

The precursor silico−alkaline solutions are composed of a distribution of different polysilicates ions. Previous works[11,12] gave a structural description of these silicate species. The structural unit of these species (dimer, trimer, cylcic hexamer, cubic octamer, etc.) is the monomeric orthosilicate anion SiO_4^{4-}, which is in a tetrahedron environment. In a recent work,[8] it

10.1021/jp990151s CCC: $18.00
Published on Web 06/24/1999

TABLE 1: Calcium Concentration Used for Destabilized Silico−Alkaline Solutions with Different Molar Ratio R_m and Different Alkaline Ions

	SiO_2-A_2O with A: alkaline									
	Li		Na		K		Rb		Cs	
R_m $[SiO_2]/[A_2O]$	2	3	2	3	2	3	2	3	2	3
$[Ca(OH)_2]$ (mol L^{-1})	0.16	0.45	0.08	0.08	0.45	0.3	0.5	0.6	0.7	0.5

was demonstrated that the fraction of the different silicate species in sols is controlled by hydroxide concentration and by the nature of the counterion, i.e., the alkaline ion. In addition, at constant hydroxide concentration, the large species are strongly stabilized by large counterions (Li^+, Rb^+, and Cs^+) while linear species by relatively small counterions (Na^+ and K^+). These results suggest the existence of strong interactions between silicate species, hydroxide ions, and alkaline ions.

The present investigation deals with the sol−gel transformation in silico−alkaline solutions destabilized by calcium addition. In a previous work,[6] it was demonstrated that the gelation time is strongly dependent on (i) the nature of alkaline ion present in the precursor solutions and on (ii) the concentration of the powdered calcium hydroxide added to the solution.

Basically, for a given silico−alkaline solution, gelation time increases for decreasing calcium concentration. This result is consistent with the features of the two reactions described before (reaction 2 and 3). For solutions with a constant calcium concentration and different alkaline ions, the gelation time increases in the following order: sodium, potassium, lithium, rubidium, and cesium. These results corroborate the importance role of alkaline and calcium ions in the process of formation of silico−calco−alkaline gels.

In the present investigation, the mechanism of gelation and the structural features of the final gel are characterized as functions of the nature alkaline ions, calcium concentration, and hydroxide ion content.

No characterization of silica gels under strong basic conditions has been previously reported.

X-ray, neutron, and light scattering techniques were often used to describe aggregation process in solutions and gelation processes. In most of the reported investigations, only one of the mentioned scattering techniques is employed. In the present investigation, the three scattering techniques are used together in order to obtain structural information within a wide length scale (2−200 nm).

II. Samples and Experimental Techniques

II.1. Sample Preparation. Different silico−alkaline sols were obtained by mixing silica (silicagel, Merck Gel de silice 60, 70-230 mesh ASTM), with alkaline oxide and water. Two sets of five sols with silica/alkaline molar ratios $R_m = 2$ and 3 were prepared. R_m is defined as the molar ratio between silica and the alkaline oxide ($R_m = [SiO_2]/[A_2O]$ with A = alkaline). Each sol of the two sets contains Li, Na, K, Rb, and Cs oxide, respectively.

Samples were mixed in PTFE containers until complete dissolution (no filtration). Silica concentration was kept constant and equal to, 1.5 mol L^{-1}, in all samples.

Concentrations of the powdered calcium hydroxide were chosen in such a way that gelation times be kept between 2 and 3 h for all solutions. This range of gelation times allows for detailed but not too long in situ (ELS, SANS, and SAXS) studies. Calcium hydroxide concentrations of different studied solutions are listed in Table 1. Just after the calcium hydroxide addition, the sols were sonicated and centrifuged during 1 min in order to obtain inititially homogeneous sols. The solutions destabilized by calcium addition were quickly placed inside the liquid sample cells in order to be studied in situ by means of the different scattering techniques.

II.2. Experimental Techniques. Small-angle X-ray Scattering (SAXS) measurements were performed at the Laboratoire pour l'Utilisation du Rayonnement Electromagnétique (LURE) in Orsay, France, using beamline D22. The X-ray beam is monochromatized using an asymmetrically cut and bent silicon (111) single crystal (wavelength $\lambda = 1.609$ Å). The crystal also focuses the beam in the horizontal plane at the detector position. The incident beam cross section is defined by three sets of slits. The scattering X-ray intensity $I(q)$ was recorded as a function of the modulus of the scattering vector q using a vertical 1D gas X-ray position sensitive detector. The samples were placed inside a 1 mm thick cell with parallel thin Kapton windows. The parasitic scattering produced by collimating slits, Kapton windows, and air was subtracted from the total measured scattering intensity. The values of the modulus of the scattering vector q in SAXS experiments range from ∼0.0067 to ∼0.4 $Å^{-1}$.

Small angle neutron scattering (SANS) measurements were performed at the Laboratoire Léon Brillouin (LLB) in Saclay, France, on the PACE spectrometer. The neutron wavelengths used were $\lambda = 15.2$ and 6.1 Å, and the sample-to-detector distance of 4.6 and 2.9 m, respectively. The q values in these experiments range from ∼0.0027 to ∼0.110 $Å^{-1}$. The total scattered intensities $I(q)$ were corrected for transmission, for scattering of the sample cell, and for a small constant instrumental background. $I(q)$ was normalized to the sample thickness and to incoherent scattering from a water standard. To prevent strong incoherent scattering from hydrogen atoms, the precursor silico−alkaline solutions were prepared using heavy water.

Elastic light scattering (ELS) experiments were performed at the Laboratoire de Recherches sur la Réactivité des Solides (LRRS) in Dijon, France, using a Malvern 4700 instrument. The source is He−Ne laser operating at a wavelength $\lambda = 633$ nm. The scattering measurement were performed for different angles θ varying from 30° up to 150°. The chosen angles θ correspond to 30 equally spaced values in a logarithmic scale. The values of the modulus of the scattering vector, $q = (4\pi n/\lambda)\sin(\theta/2)$, were determined using a refraction index $n = 1.33$. The values of q in this ELS experiment range from ∼0.00023 to ∼0.0022 $Å^{-1}$. Scattering intensities were recorded using a standard photomultiplier and background effects were subtracted.

SANS measurements were carried out in order to record the scattering intensity within a q interval which fills the gap between the q ranges covered by ELS and SAXS. In all shown scattering curves, the results obtained by ELS, SANS, and SAXS are plotted together. To obtain a continuous curve in the whole q range, the parts corresponding to the results concerning each one of the different techniques were multiplied by appropriate scale factors.

III. Results

III.1. Scattering Produced by Gels. The experimental scattering intensity curves corresponding to different gels formed

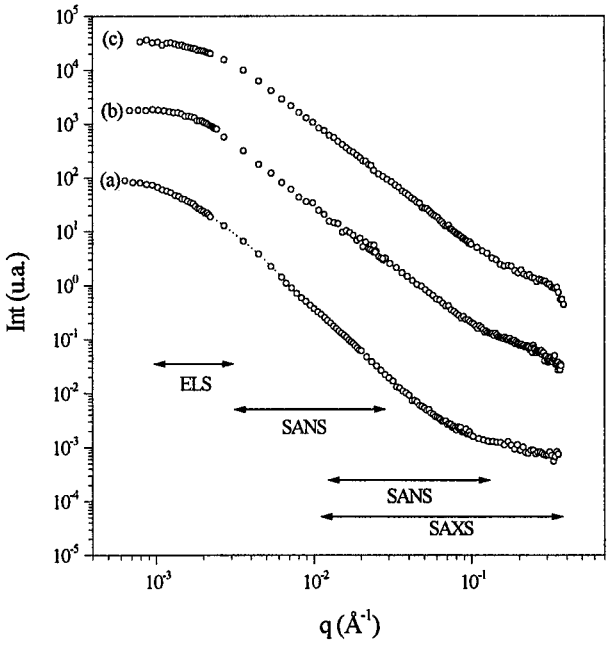

Figure 1. Experimental scattering curves corresponding to basic silica gels formed from silico−alkaline precursor solutions destabilized by a low addition of calcium. (a) $t = 60$ mn, $SiO_2/Na_2O = 2 + [Ca(OH)_2] = 0.08$ mol L^{-1}; (b) $t = 120$ mn, $SiO_2/Na_2O = 3 + [Ca(OH)_2] = 0.08$ mol L^{-1}, and (c) $t = 150$ mn, $SiO_2/Li_2O = 2 + [Ca(OH)_2] = 0.16$ mol L^{-1}.

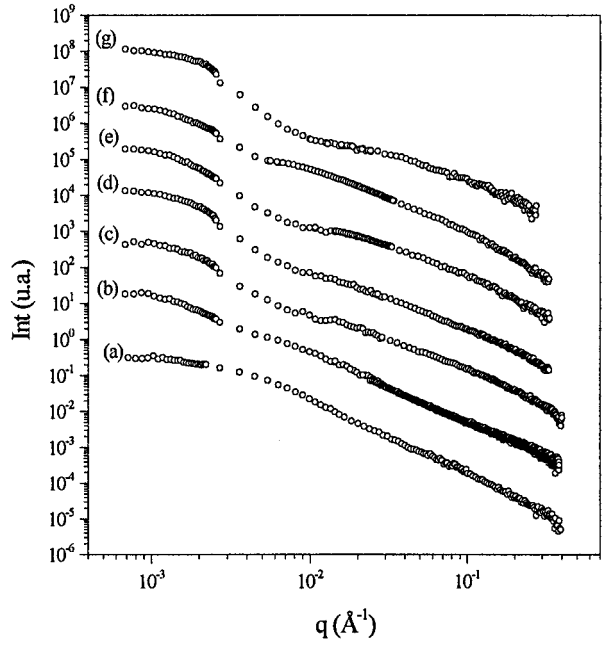

Figure 2. Experimental scattering curves at $t = 150$ min corresponding to basic silica gels formed from silico−alkaline precursor solutions destabilized by a high addition of calcium. (a) $SiO_2/K_2O = 3 + [Ca(OH)_2] = 0.3$ mol L^{-1}, (b) $SiO_2/K_2O = 2 + [Ca(OH)_2] = 0.45$ mol L^{-1}, (c) $SiO_2/Li_2O = 3 + [Ca(OH)_2] = 0.45$ mol L^{-1}, (d) $SiO_2/Rb_2O = 2 + [Ca(OH)_2] = 0.5$ mol L^{-1}, (e) $SiO_2/Cs_2O = 3 + [Ca(OH)_2] = 0.5$ mol L^{-1}, (f) $SiO_2/Rb_2O = 3 + [Ca(OH)_2] = 0.6$ mol L^{-1}, and (g) $SiO_2/Cs_2O = 2 + [Ca(OH)_2] = 0.7$ mol L^{-1}.

from silico−alkaline precursor solutions are plotted in Figures1 and 2. Ten sets of three scattering curves were recorded using ELS, SANS, and SAXS. The different q ranges corresponding to each one of the three techniques are reported in Figure 1.

A preliminary qualitative analysis of Figures 1 and 2 indicates that the scattering curves can be classified in two sets with

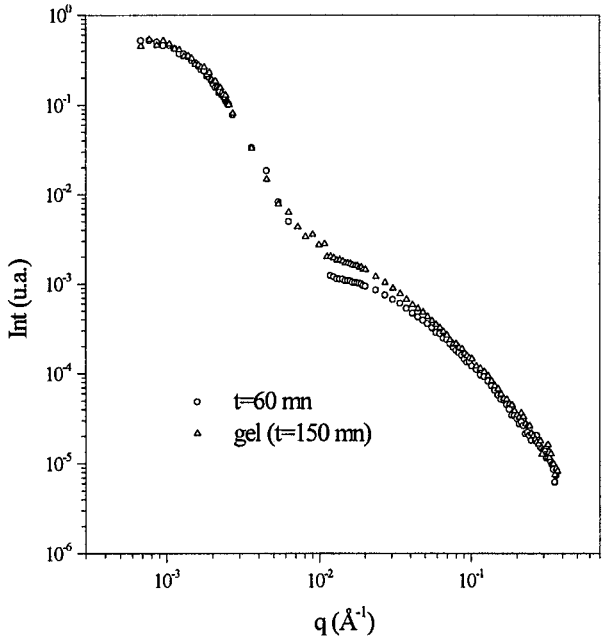

Figure 3. Experimental scattering curves corresponding to different periods of time during aggregation and formation of a gel derived from lithium silicate precursor solutions with silica/alkaline ratios $R_m = 3$ and $[Ca(OH)_2] = 0.45$ mol L^{-1}.

clearly different features, corresponding to low and high calcium concentration, regardless of the nature and concentration of alkaline, i.e., molar ratio. Therefore, it became apparent that the only important parameter determining the relevant structural features of the gels is calcium concentration.

The scattering curves plotted in Figure 1, corresponding to low calcium concentration ($[Ca(OH)_2] < 0.3$ mol L^{-1}), exhibit a simple q dependence, qualitatively similar to those previously reported in the literature for a number of other gels. The results shown in Figure 2 are more complex and suggest a bimodal particle size distribution for high calcium concentration ($[Ca(OH)_2] \geq 0.3$ mol L^{-1}).

III.2. Kinetic of Gel Formation in Samples with High and Low Calcium Concentrations. Figures 3 and 4 correspond to scattering intensity produced by two solutions with high and low calcium concentrations, respectively, both evolving from solution to gel state. These series of scattering curves were recorded in situ as a function of time during aggregation in solution and until the gel state.

The sequence of scattering curves corresponding to different increasing times under isothermal conditions, corresponding to high calcium concentration, does not exhibit important variations. Two of the recorded scattering curves are plotted in Figure 3 in log−log scale. The two shoulders in the curves suggest, as specified before, the presence of scattering objects with a well-defined bimodal size distribution. These features are apparent from the beginning of aggregation in the solution, i.e., in this figure at $t = 60$ mn, up to the formation of the final gel.

The scattered intensity from isolated and not strongly correlated particles or fractal aggregates may be approximated in the limit of small q by[13,14]

$$I(q) = I(0)\exp\left(-\frac{R_g^2 q^2}{3}\right) \quad (1)$$

R_g being the "Guinier average" of the radius of gyration of the scattering objects. In the case of gels formed by clustering of

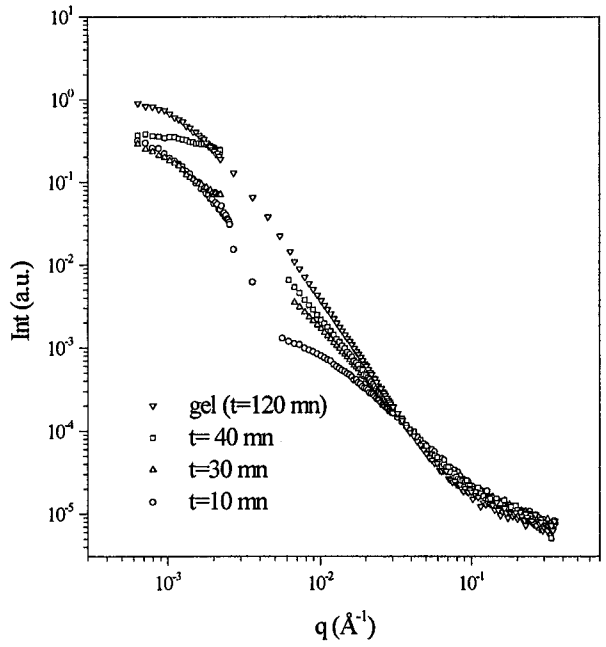

Figure 4. Experimental scattering curves corresponding to different periods of time during aggregation and formation of a gel derived from sodium silicate solutions with silica/alkaline ratios $R_m = 3$ and [Ca(OH)$_2$] = 0.08 mol L^{-1}.

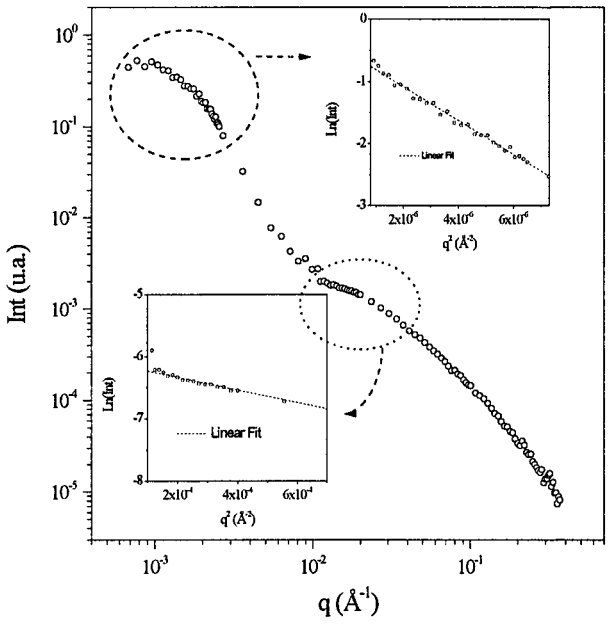

Figure 5. Experimental scattering curve and Guinier plots in two q domains (insets) corresponding to the first moment of aggregation (curve Figure 3 for $t = 60$ mn). The precursor system is a lithium silicate solution with silica/alkaline ratios $R_m = 3$ and [Ca(OH)$_2$] = 0.45 mol L^{-1}.

fractal objects, their average size is characterized by the correlation length ξ.

Guinier plots of the scattering curves produced by samples with high calcium concentration are shown in the insets of Figure 5. The scattering curves exhibit a linear dependence in two q domains ($1 \times 10^{-6} < q^2 < 7 \times 10^{-6}$ Å^{-2} and $1 \times 10^{-4} < q^2 < 7 \times 10^{-4}$ Å^{-2}). The Guinier averages of the radii of gyration of the aggregates R_g, determined from the slopes of the straight lines within the low q and high q ranges of linearity, are equal to 800 and 80 Å, respectively. Similar values were obtained from the scattering results corresponding to the final gels.

The scattering curve, in log−log scale, corresponding to initial states of aggregation in samples with low calcium concentration (Figure 4, curve $t = 10$ mn) exhibits a q dependence similar to that observed for all samples with high calcium concentration (Figure 3). However, in the case of low calcium concentration, the scattering curve (Figure 4) evolves with time and progressively modifies its shape until the final gel state is reached. The overall q dependence of the experimental scattering intensity suggests that gels are predominantly composed of aggregates with a single mode size distribution.

The log−log plots of $I(q)$, corresponding to the gel state of samples with high (Figure 3) and low (Figure 4) calcium concentrations, both exhibit well-defined domains of linear dependence. The q range of linear dependence for low calcium is much wider than for high calcium content. In the case of high calcium content, linearity is apparent only in the range $0.02 < q < 0.10$ Å^{-1}, corresponding to the mode of rather small aggregates.

In addition to the features mentioned above, the tails of the scattering curves produced by gels with low calcium concentration at high q ($q > 10^{-1}$ Å^{-1}), shown in Figure 4, exhibit a positive deviation from their linear behavior. This effect was assigned to a contribution to scattering intensity produced by residual isolated particles remaining from the solution, so indicating the existence of residual particles of solution also in the solution remaining in the pores of the gel phase. This effect in the tails of scattering intensity is not apparent in the $I(q)$ function corresponding to samples with high calcium concentration (Figure 3).

III.3. Fractal Dimension *D* as a Function of Calcium Concentration and Molar Ratio. *III.3.1. Theoretical Model.* Materials composed of monodisperse and isolated objects or particles embedded in a homogeneous matrix, produce a (light, neutron or X-ray) scattering intensity $I(q)$ given by

$$I(q) = \phi P(q) S(q) \tag{2}$$

where ϕ is the number density of particles, $P(q)$ is the primary particle form factor and $S(q)$ is the structure function which accounts for interference effects on scattering intensity produced by particle spatial correlation.

In the simple case of spherical particles with radius R, volume V, and uniform electronic density ρ embedded in a matrix with density ρ_0, $P(q)$ is given by[13,15]

$$P(q) = [V(\rho - \rho_0)]^2 \left[3\frac{\sin(qR) - qR\cos(qR)}{(qR)^3}\right]^2 \tag{3}$$

Teixeira et al.[16−19] theoretically analyzed the structure function associated to a finite fractal object composed of primary particle characterized by a size parameter R with an overall correlation length ξ. This function is given by

$$S(q) = 1 + \frac{1}{(qR)^D}\frac{D\Gamma(D-1)}{[1 + 1/(q^2\xi^2)]^{(D-1)/2}}\sin[(D-1)\tan^{-1}(q\xi)] \tag{4}$$

Γ being the gamma function and D the fractal dimension of the structure.

In case of a fractal object with an overall correlation length ξ much larger than the radius of primary particles R, the log−log plot of $S(q)$ exhibits three linear domains corresponding to

$q \ll 1/\xi$, $1/\xi \ll q \ll 1/R$ and $q \gg 1/R$ and two crossovers at $q = 1/\xi$ and $q = 1/R$.

The theoretical expressions for the scattering intensity (eq 2) applies to fractal objects formed by aggregation of primary particles with equal sizes. In the solutions studied in this work, the primary particles are polysilicates with different degree of polymerization, their average radii ranging from 3 to 10 Å.[8] Even though the condition about the equivalent size of the primary particles is not satisfied, we applied eqs 2, 3, and 4 as a first approximation to our experimental results.

On the other hand, the primary particles being much smaller than the aggregates, the form factor $P(q)$ was considered as a constant within the q range of our experiments. Under this condition, the scattering intensity $I(q)$ produced by fractal objects becomes proportional to the structure function $S(q)$ given by eq 4.

The deviation from linearity of the scattering intensity in log−log plots at high q (Figure 1) was assigned to the scattering produced by residual primary particles still in solution inside the pores of gels with low calcium content. By combining previous experimental results using ^{29}Si nuclear magnetic spectroscopy data and SAXS measurements,[8] the scattering intensity curves corresponding to the silico−alkaline solutions, $I_{sol}(q)$ were calculated.

The scattering intensity produced by a system composed of fractal aggregates and small primary particles, with negligible spatial correlation between them, is given by

$$I(q) = I_1 + BI_{sol} \tag{5}$$

$I_1(q)$ being the intensity produced by the fractal aggregates and $BI_{sol}(q)$ the scattering intensity produced by the small primary particles remaining in the solution inside the pores of the wet gel.

III.3.2. Fitting of Theoretical Functions to Experimental Results. All scattering curves corresponding to gel states for samples with low calcium concentration exhibit a linear behavior in log I versus log q plots within a wide q-range (Figure 1). This behavior is expected for fractal objects with an average correlation length much larger than the size of the primary particles ($\xi \gg R$).

Figure 6 illustrates the fittings of eq 5, including the contribution from the isolated particles remaining from the solution, to the experimental data corresponding to three samples with low calcium: (i) Na and $R_m = 2$, (ii) Na and $R_m = 3$, and (iii) Li and $R_m = 2$. The fitting of eq 5 to the experimental data yielded the dimension D and the correlation length ξ of the fractal objects shown in Figure 8. The different values of the fractal dimension D (Figure 8) lie between 2.2 and 2.5.

The scattering intensity functions, produced by samples with high calcium content, are displayed in Figure 7, in log−log scale. A linear dependence of log $I(q)$ is apparent within a rather narrow q range ($0.02 < q < 0.10$ Å^{-1}). The small q range in which the contribution of large species is predominant is excluded in the fitting of eq 4 to the experimental data. The values of D (Figure 8) corresponding to all the studied samples with high calcium content lie between 1.7 and 1.95.

The different values of fractal dimension associated to samples with high and low calcium content (1.7−1.95 and 2.1−2.5, respectively) suggest that the mechanism responsible for particle aggregation strongly depends on calcium concentration and is nearly insensitive to the nature of the alkaline ion.

IV. Discussion

IV.1. Large Particles Formed at the Beginning of Aggregation. The formation of large particles (average diameter of about 800 Å) occurs at a very early stage of aggregation, just after calcium addition, either in samples with high and low calcium concentration. The very fast growth of large particles seems to be related to the existence of an extremely high calcium concentration close to the hydroxide calcium solid particles just after their addition. After homogenization of the sol, the growth of these large particles stops and their size remain since then essentially invariant. The scattering produced at small q by these large particles remains nearly constant from the beginning of aggregation until the gel final state. The small q scattering produced by these large particles remains constant until the gel state.

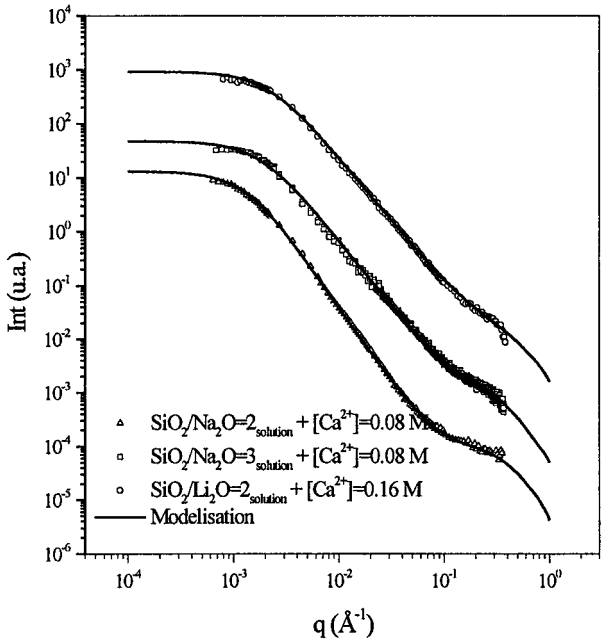

Figure 6. Experimental and theoretical curves, fitted using eq 5, corresponding to a gel with a low calcium concentration.

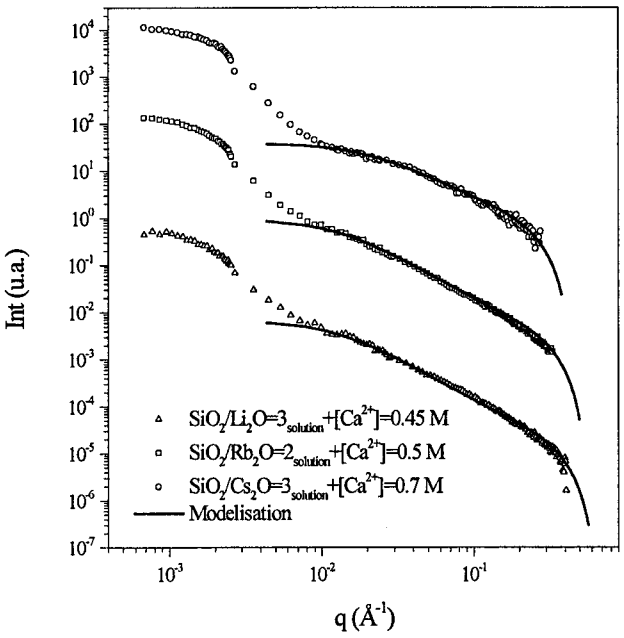

Figure 7. Experimental and theoretical curves, fitted using eq 4, corresponding to a gel with high calcium concentration. The theoretical curves were fitted to the experimental intensity excluding the contribution in the low q range from the large particles formed just after calcium addition.

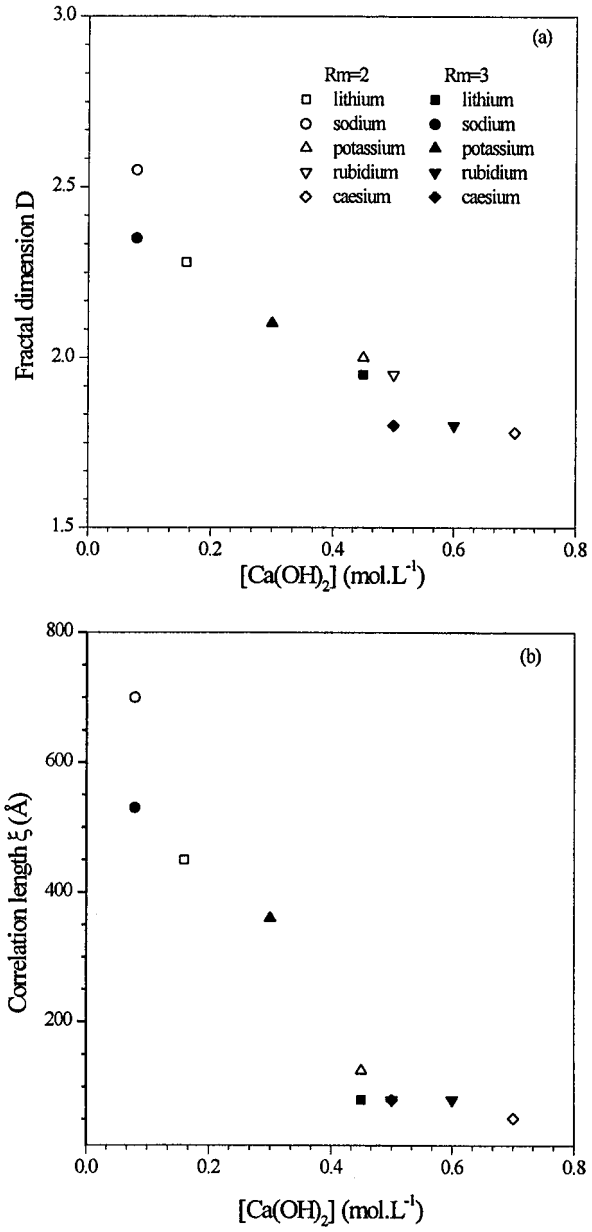

Figure 8. (a) Fractal dimension D and the (b) overall size ξ in function of the hydroxide calcium concentration.

IV.2. Fractal Aggregates and Aggregation Mechanisms. In samples with high calcium concentration, the fractal aggregates stop their growth when they are rather small (with a correlation length of about 80 Å). So the much larger particles formed in the solutions just after calcium addition yield a predominant contribution to the scattering intensity at small q, at the beginning of aggregation and also during and after the formation of the gel phase. So the particle size distribution remains bimodal during the whole processes of gel formation.

In samples with low calcium concentration, the fractal aggregates grow much more than in those with high calcium, their size becoming comparable to that of the large particles described in IV.1. So, the fractal aggregates contribute to the scattering intensity in the whole q range of the experiments. For the gel state, the experimental scattering intensity is mainly produced by fractal aggregates, with a minor contribution at high q from isolated primary particles. This implies that, at advanced stages of aggregation, the large particles are less numerous than fractal aggregates, so giving a comparatively negligible contribution to scattering intensity.

The scattering results corresponding to low calcium samples in gel state also indicate that small primary particles of the precursor solution remain embedded in the pores and coexist with the gel network.

Many investigations using computer simulation were carried out in the past decades in order to correlate the mechanism involved in aggregation and the fractal dimension of the aggregates. One of the models assumes an immobile cluster progressively growing by aggregation of monomer particles. For this model, named diffusion-limited aggregation (DLA) or particle-cluster aggregation, Witten and Sanders[20] obtained a fractal dimension $D = 2.5$. Later on, a number computer simulations[21−23] dealt with two other models named diffusion limited cluster aggregation (DLCA) and Reaction Limited Cluster Aggregation (RLCA). In these models a large number of clusters progressively grow by sticking one to each other as well as by monomer addition. The fractal dimensions determined for these models are1.75−1.80 for DLCA and 2.11 for RLCA. Higher values of fractal dimension can be qualitatively associated to denser structures. For RLCA the clusters are in contact many times before they stick. The origin of the low sticking probability may be chemical or associated to electrostatic physical interactions.

The experimental values of D obtained from our experimental scattering results, corresponding to the different systems with high and low calcium concentration, were compared with those deduced for the described theoretical models. For different gels with high calcium content, the fractal dimension determined experimentally lie between 1.8 and 2.0, so the most probable mechanism is DLCA. For different gels with low calcium concentration, the experimental dimension lie between $D = 2.1-2.5$, these values being closer to the computer simulation results for DLA and RLCA.

For high calcium content, the experimental fractal dimension $D = 1.8-2.0$ reflects the stringy nature of the clusters and corresponds to the mechanism DLCA. This seems justified because the number of calcium ions in solution being high, the sticking probability of two silicate species is very much enhanced. If we consider that primary particles and clusters aggregate every time they meet, the controlling mechanism for aggregation becomes diffusion in liquid phase.

For low calcium concentration, the fractal dimension ranges from 2.1 to 2.55. These values may correspond, in principle, either to RLCA and DLA models. However, DLA[20] (immobile clusters growing by monomer addition) seems an unrealistic model to be applied to our system which consists of a large number of growing clusters embedded in a liquid medium. In addition, these higher values of fractal dimension could not be interpreted as an aging effect because the gel is just formed. On the other hand, when calcium concentration is low, the small number of calcium ions reduces the sticking probability of silicate species. Therefore, in this case, silicate particles will not stick every time that they meet, which is the basic assumption for RLCA. Therefore, we conclude that RLCA is the controlling mechanism for gelation in sols with low calcium content. This mechanism promotes the diffusion of particles inside the fractal structure and, consequently, the formation of denser structures with higher fractal dimension.

V. Conclusion

This investigation demonstrates that the concentration of calcium ions is the main factor that controls aggregation and

gelation processes in silico−alkaline solutions. The presented results suggest that aggregates grow by reaction limited cluster aggregation in systems with low calcium and by diffusion-limited cluster aggregation in samples with high calcium concentration.

The structure of the studied gels is also strongly dependent on calcium concentration. As a matter of fact, solutions with a high calcium concentration yield gels composed of rather small fractal aggregates and large particles formed just after calcium addition. On the other hand, solutions with low calcium content induce the formation of gels mainly composed of large fractal aggregates coexisting with small primary silicate species.

The mechanism of particle growth and the structure of the final gels are not noticeably modified, neither by the nature of the alkaline ions nor by their molar ratio.

This investigation demonstrated the usefulness of ELS, SANS, and SAXS techniques when applied together to study solutions and gels. They allowed for the simultaneous characterization of coarse structural entities (the large particles), fractal aggregates, and small primary species. It was also possible to determine the connection between the structure of the aggregates and gels and the conditions under which chemical reactions take place.

Acknowledgment. The authors thank Dr. Loic AuVray (LLB, Saclay, France) for many helpful suggestions in neutron scattering experiments.

References and Notes

(1) Iler, R. K. *The Chemistry of Silica*; John Wiley & Sons: New York, 1979.

(2) Brinker, C. J.; Scherer, G. W. *Sol−Gel Science: The Physics and Chemistry of Sol−Gel Processing.*; Academic Press: New York, 1990.

(3) Bolt, P. H.; Dokter, W. H.; Beelen, T. P. M.; Van Santen, R. A. *SPIE* **1997**, *3095*, 174.

(4) Beelen, T. P. M.; Wijnen, P. W. J. G.; Vonk, C. G.; Van Santen, R. A. *Catal. Lett.* **1989**, *3*, 209.

(5) Wen, Z. Formation et caractérisation de sols alcalins de silice. Conditions de leur transformation en gel au contact de sels et d′hydroxydes, notamment de ceux qui sont présents dans le béton. Etude particulière du role de la portlandite. Ph.D. Thesis, Université de Bourgogne, 1989.

(6) Gaboriaud, F.; Chaumont, D.; Nonat, A.; Hanquet, B.; Craievich, A. *J. Sol−Gel Sci. Technol.* **1998**, *13*, 353.

(7) Dent Glasser, L. S.; Kataoka, N. *Cem. Concr. Res.* **1981**, *11*, 1.

(8) Gaboriaud, F.; Nonat, A.; Chaumont, D.; Craievich, A.; Hanquet, B. *J. Phys. Chem. B* **1999**, *103*, 2091.

(9) Michaud, V.; Nonat, A.; Sorrentino, D. "Experimental Simulation of Mechanisms Involved in the Building of Stresses in Concretes Subjected to Alkali−Silica Reaction"; Proceedings of the 10th International Congress on the Chemistry of Cement, Gothenburg, 1997.

(10) Nieto, P.; Dron, R.; Thevenot, R.; Zanni, H.; Brivot, F. *C. R. l'Acad. Sci. Paris* **1995**, *320*, 485.

(11) Harris, R. K.; Newman, R. H. *J. Chem. Soc., Faraday Trans.* **1977**, *2*, 1204.

(12) Engelhardt, G.; Michel, D. *Hight-Resolution Solid-State NMR of Silicates and Zeolites*; John Wiley & Sons: New York, 1987.

(13) Guinier, A. *X-ray Diffraction in Crystals, Imperfect Crystals, and amorphous Bodies*; Dover Publications: New York, 1994.

(14) Kratky, O.; Laggner, P. X-ray small angle scattering. In *Encyclopedia of Physical Science and Technology*; Academic Press: New York, 1992; Vol. 17, p 727.

(15) Debye, P. *Phys. Z.* **1927**, *28*, 135.

(16) Teixeira, J. *J. Appl. Crystalogr.* **1988**, *21*, 781.

(17) Teixeira, J. Introduction to small angle neutron scattering apllied to colloidal science. In *Structure and Dynamics of Strongly Interacting Colloids and Supramolecular Aggregates in Solution*; Chen, S.-H., et al., Ed.; Kluwer Academic Publishers: Netherlands, 1992; p 635.

(18) Chen, S.-H.; Teixeira, J. *Phys. Rev. Lett.* **1986**, *57*, 2583.

(19) Sinha, S. K.; Freltoft, T.; Kjems, J. Observation of power-law correlations in silica-particle aggregates by small-angle neutron scattering. In *Kinetics of Aggregation and Gelation*; Family, F., Landau, D. P., Eds.; Elsevier: Amsterdam, 1984; p 87.

(20) Witten, T. A.; Sander, L. M. *Phys. Rev. Lett.* **1981**, *47*, 1400.

(21) Kolb, M.; Jullien, R. *J. Phys.,-Lett.* **1984**, *45*, L.

(22) Brown, W. D.; Ball, R. C. *J. Phys. A Generalities* **1985**, *18*, L517.

(23) Meakin, P. *J. Colloid Interface Sci.* **1984**, *102*, 491.